


Cite this: *RSC Adv.*, 2019, 9, 22064

# Increased expression of core-fucosylated glycans in human lung squamous cell carcinoma

Tianran Ma,<sup>a</sup> Yan Wang,<sup>a</sup> Liyuan Jia,<sup>a</sup> Jian Shu,<sup>a</sup> Hanjie Yu,<sup>a</sup> Haoqi Du,<sup>a</sup> Jiajun Yang,<sup>a</sup> Yiqian Liang,<sup>b</sup> Mingwei Chen<sup>\*b</sup> and Zheng Li<sup>id</sup> <sup>\*a</sup>

Lung cancer is the most frequent cancer and the leading cause of cancer around the world. As one of the major types of lung cancer, lung squamous cell carcinoma (LUSC) is closely associated with smoking and shows poor sensitivity to therapy and prognosis. Although alteration of glycopatterns are reliable indicators of cancer, little is known about the alterations of protein glycosylation related to LUSC. In this study, we compared the differential expression levels of glycopatterns in seven pairs of LUSC tissues and normal pericarcinomatous tissues (PCTs) using lectin microarrays. Fluorescence-based lectin histochemistry and lectin blotting were utilized to validate and assess the expression and distribution of certain glycans in LUSC tissues and PCTs. And we further analyzed their total *N*-linked glycans using MALDI-TOF/TOF-MS to provide more information about the aberrant glycopatterns. The results showed that the expression level of the core fucosylation recognized by *Pisum sativum* agglutinin (PSA) and *Lens culinaris* agglutinin (LCA) was significantly increased in LUSC tissues compared with PCTs. There were 10 and 15 fucosylated *N*-linked glycans that were detected in PCTs and LUSC tissues respectively, 10 fucosylated *N*-glycans were common, while five fucosylated *N*-glycans were unique to LUSC tissues. And the abundance of the fucosylated *N*-glycans was increased from 40.9% (PCTs) to 48.3% (LUSC). These finding is helpful to elucidate the molecular mechanisms underlying the lung diseases and develop new treatment strategies.

Received 10th June 2019  
Accepted 8th July 2019

DOI: 10.1039/c9ra04341a

rsc.li/rsc-advances

## 1. Introduction

Lung cancer is the major malignant tumor with the highest incidence and mortality in both sexes around the world; there were about 2.1 million new lung cancer cases and 1.8 million deaths predicted in 2018.<sup>1</sup> Lung cancer can be classified into four major histologic types of lung squamous cell carcinoma (LUSC), adenocarcinoma, small cell carcinoma, and large cell carcinoma.<sup>2,3</sup> As the major types of lung cancer, LUSC is associated with smoking and represents approximately 30% of all cases of non-small cell lung cancer.<sup>4,5</sup> Although kinase inhibitors (targeting epidermal growth factor receptor, anaplastic lymphoma kinase and c-ros oncogene 1) and immune checkpoint inhibitors (anti-programmed cell death 1 antibodies, anti-programmed cell death ligand 1 antibodies, atezolizumab and durvalumab) have been widely used in clinical practices according to the aberrant status of the cancer, it still a quite limited number of LUSC cases that were actually suitable and efficient for these treatment strategies.<sup>6–10</sup> It is still an urgent requirement to investigate the definite molecular mechanism and

antitumor treatment strategies of LUSC.<sup>11,12</sup> Therefore, identification of the difference between tumor tissues and adjacent tissues is very meaningful for contributing to the molecular mechanism research.

Glycosylation is one of the most ubiquitous and crucial post-translational modifications, occurring on virtually all known proteins in mammalian cells and involving in almost all important biological processes.<sup>13</sup> The alteration of the glycosylation occupancy or specific glycan structures are often detected during inflammation, infection, neoplastic transformation and cancer.<sup>13,14</sup> One of the most important types of glycosylation, core fucosylation is only catalyzed by fucosyltransferase 8 (FUT8).<sup>15,16</sup> Evidences showed that the increased expression level of the core fucosylation is detected in variety of disease, such as chronic pancreatitis, hepatocellular carcinoma and inflammatory bowel disease.<sup>17–19</sup> And the up-regulation of FUT8, also has been observed in several cancers including colorectal cancers, brain cancer, and lung cancer.<sup>20–22</sup> Although the FUT8 as a functional regulator of non-small cell lung cancer is revealed,<sup>22</sup> the correlation between aberrant glycans and LUSC is still no clear. Therefore, exploring the glycopatterns of LUSC tissues is also necessary to research the pathogenesis of LUSC.

In this study, the glycopatterns of seven pairs of lung tissues including tumor and normal pericarcinomatous tissues (PCTs) obtained from LUSC patients were detected using the lectin microarrays. The results were verified by fluorescence-based lectin

<sup>a</sup>Laboratory for Functional Glycomics, College of Life Sciences, Northwest University, No. 229 Taibai Beilu, Xi'an 710069, China. E-mail: zhengli@nwnu.edu.cn; Fax: +86-29-88303572; Tel: +86-29-88304104

<sup>b</sup>Department of Respiratory and Critical Care Medicine, The First Affiliated Hospital of School of Medicine of Xi'an, Jiaotong University, Xi'an 710061, China. E-mail: chenmw36@163.com



blotting and histochemistry. Furthermore, the total *N*-linked glycans were identified using MALDI-TOF/TOF-MS to provide more information about the aberrant glycopatterns between PCTs and LUSC tissues. This study provides the comprehensive information of glycopatterns from lung LUSC tissues and PCTs, which is helpful to elucidate the molecular mechanisms underlying the lung diseases and develop new treatment strategies.

## 2. Materials and methods

### 2.1 Clinical specimens

The collection and use of all human pathological specimens for the research presented here were approved by the Ethical Committee of the First Affiliated Hospital of Xi'an Jiao Tong University and Northwest University in Xi'an, China. All patients enrolled in the study provided written informed consent. This study was conducted in accordance with the ethical guidelines of the Declaration of Helsinki.

Seven pairs of lung tissues including normal PCTs and tumor tissues were obtained from seven LUSC patients, who had no history of treatment before their operation in the First Affiliated Hospital of Xi'an Jiao Tong University (Xi'an, China). Detailed information on patients is described in Table 1. The lung tissues were obtained during surgical resection and were snap-frozen in liquid nitrogen before being stored at  $-80^{\circ}\text{C}$  until required for use. PCTs were collected at a distance of at least 5 cm from the cancer lesions. All the tissues were histologically examined and were confirmed by experienced pathologists. Tissue microarrays which comprised of paraffin-embedded LUSC tissues and PCTs were purchased from Shanghai Outdo Biotech Co. Ltd. (Shanghai, China).

### 2.2 Tissue protein extraction

The total protein of lung tissue was extracted with T-PER (Thermo Scientific, Herts, UK) according to the manufacturer's instructions. Approximately 30 mg of lung tissue was homogenized in a mixer on ice in 1 mL of T-PER containing a 1% protease inhibitor cocktail

(complete, EDTA-free, Roche, Basel, Switzerland). Following centrifugation at  $10\,000g$  for 5 min, the supernatant was immediately transferred for use or stored at  $-80^{\circ}\text{C}$ . The protein concentration was determined using a BCA assay.

### 2.3 Lectin microarrays and data analysis

The lectin microarrays were produced using 37 lectins with different binding preferences covering *N*- and *O*-linked glycans. The Cy3-labeled proteins were incubated in the lectin microarrays to detect the different glycopatterns among clinical samples. The lectin microarrays were produced according to the protocol.<sup>23</sup>

### 2.4 Lectin blotting

To normalize the differences between subjects and to tolerate individual variation, samples in each group were pooled, respectively. The expression level of specific glycans was further analyzed by lectin blotting according to the protocol.<sup>24</sup> The pooled tissue proteins of each group were subjected to 10% SDS-PAGE electrophoresis, and transferred to PVDF membranes incubated with Cy5-labeled PSA and LCA.

### 2.5 Real-time quantitative PCR

RNA isolation, cDNA synthesis and quantitative real-time polymerase chain reaction (qRT-PCR) were described in the previous manuscript.<sup>25</sup> The gene specific primers used in this study including FUT8 (F: 5'-AACTGGTTCAGCGGAGAATAACR-3'; R: 5'-TGAGATTCCAAGATGAGTGTTCG-3'); and GAPDH (F: 5'-GGAGCGAGATCCCTCCAAAT-3'; R: 5'-GGCTGTTGTCA-TACTTCTCATGG-3'). The mRNA levels of the genes were normalized to the amount of GAPDH in each sample, and quantization of gene expression level was determined using the  $2^{-\Delta\Delta C_T}$  comparative method.

### 2.6 Fluorescence-based lectin histochemistry

Cy3-labeled lectins were applied to detect the specific glycan structures present on the lung tissue sections as described.<sup>24</sup>

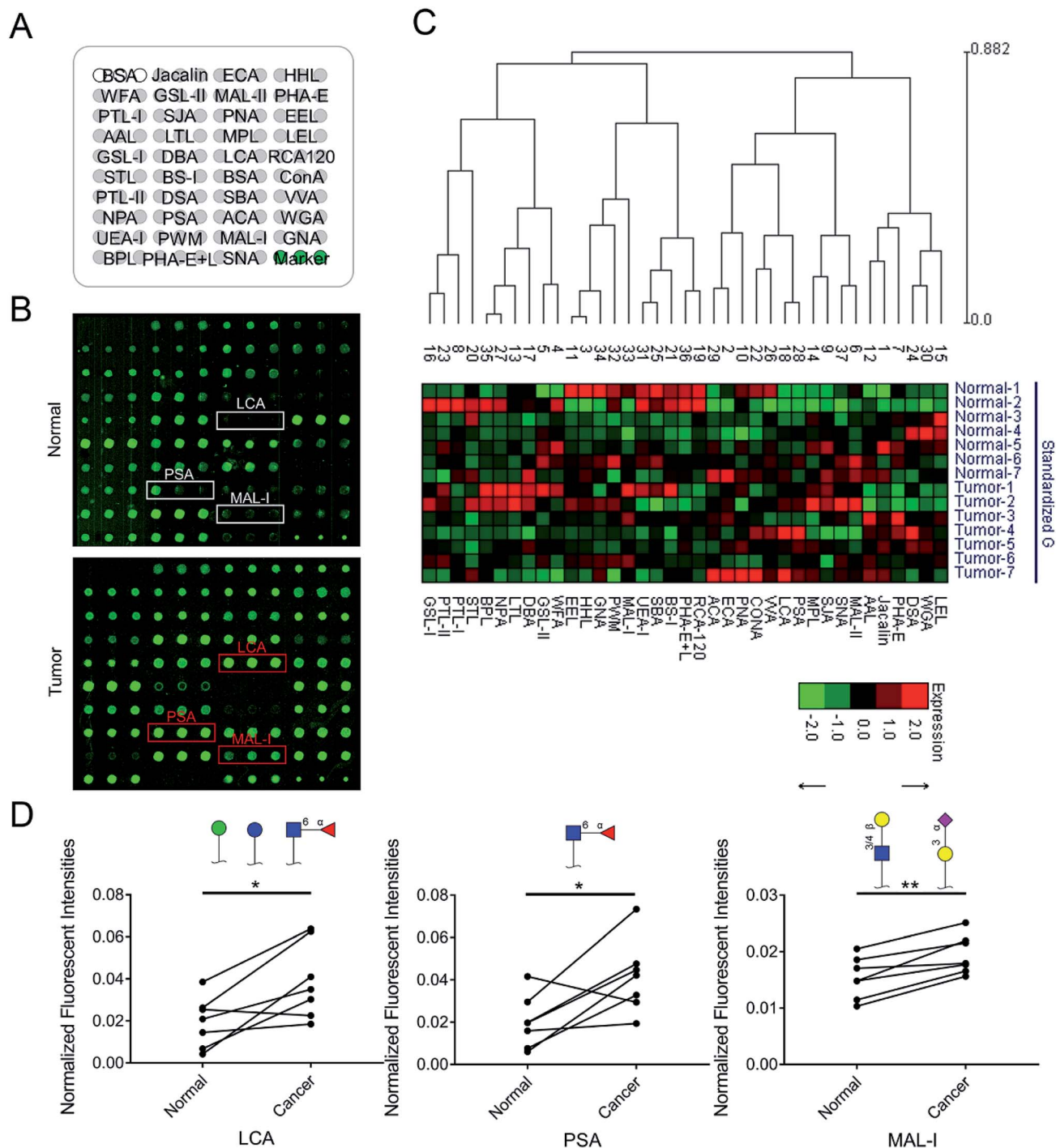
**Table 1** Clinical characteristics of patients and the normalized fluorescent intensities (NFIs) of the altered lectins

Patient no.		1	2	3	4	5	6	7
Gender		Male	Male	Male	Female	Male	Male	Male
Age, years		57	66	52	62	63	61	54
Smoking index		—	1500	300	—	300	900	700
AJCC staging		IIB	IIA	IB	IIA	IA	IIA	IIB
Lectin	NFIs							
LCA	N	0.007	0.004	0.015	0.026	0.021	0.025	0.039
	T	0.030	0.041	0.018	0.063	0.035	0.023	0.064
PSA	N	0.008	0.006	0.016	0.030	0.020	0.042	0.020
	T	0.033	0.042	0.019	0.073	0.045	0.029	0.048
MAL-I	N	0.021	0.011	0.015	0.010	0.015	0.019	0.017
	T	0.025	0.017	0.022	0.016	0.018	0.022	0.018



Briefly, formalin-fixed paraffin-embedded tissue microarrays were dewaxed and hydrated in a series of different concentrations of dimethylbenzene and ethanol. The tissue microarrays were rinsed 3 times with PBS for 5 min and blocked with blocking buffer (PBS supplemented with 5% BSA) at 25 °C for 30 min. Thereafter, the sections were incubated with a solution

containing a final concentration of 100  $\mu\text{g mL}^{-1}$  Cy3-labeled lectins and 5% (w/v) BSA for 3 h at room temperature, in the dark. Finally, sections were stained with DAPI (1  $\mu\text{g mL}^{-1}$  in PBS; Roche) for 10 min before the final rinse. A laser scanning confocal microscope FV 1000 (Olympus, Tokyo, Japan) was used to collect the images using the merge channels of Cy3 and DAPI.



**Fig. 1** The glycopatterns of PCTs and LUSC tissues. (A) Layout of the lectin microarray. Each lectin was spotted in triplicate per block, with triplicate blocks per slide. Cy3-labeled BSA was spotted as a location marker and unlabeled BSA as a negative control. (B) Glycopattern of PCTs (up) and LUSC tissues (down) detected by the lectin microarray. Red frames marked lectins showing significant increase between PCTs and tumor tissues. (C) Hierarchical clustering and the relative binding intensities of the 37 lectins in the two groups from 7 patients. (D) The significant difference of glycopatterns between PCTs and LUSC tissues.

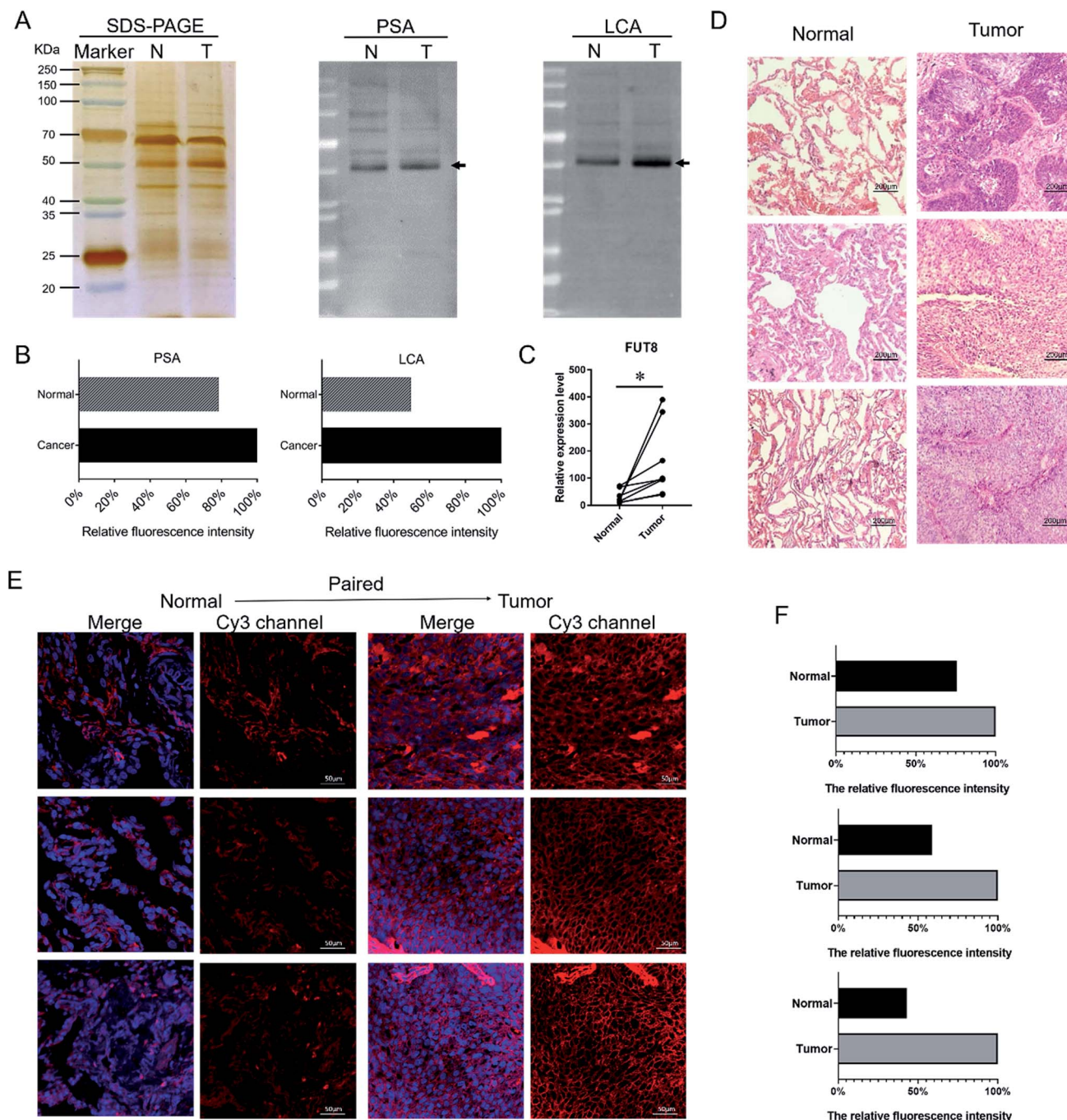




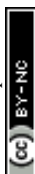
## 2.7 Isolation and purification of N-linked glycans

The N-glycans released by PNGase F glycosidase (New England Biolabs, Beverly, MA) according to previous protocols.<sup>26</sup> Briefly, 200  $\mu$ g glycoproteins were concentrated and desalted by adding to a 3K centrifugal ultrafiltration. Then, the obtained

glycoproteins were denatured with 8 M urea, 10 mM DTT and 10 mM IAM, and exchanged buffer into 40 mM  $\text{NH}_4\text{HCO}_3$  by using 3K centrifugal ultrafiltration. After that, 2  $\mu$ g trypsin was added to digest the glycoproteins overnight at 37 °C. The mixture was heated at 80 °C for 5 min to deactivate the activity



**Fig. 2** Validation of the differential expressions of the glycoproteins in PCTs and LUSC tissues. (A) The binding pattern of glycoproteins from PCTs and LUSC tissues using PSA and LCA. The major increased fluorescence intensities glycoproteins located in the band with approximately 53 kDa. N, normal (PCTs); T, tumor (LUSC). (B) The fluorescence intensities of the major difference bands were read by ImageJ and showed by relative value in the histogram. (C) The FUT8 was increased in the LUSC tissues compared with the PCTs. (D) The H&E staining of PCTs and LUSC tissues. (E) Increased expression and location of the core fucosylation glycans in PCTs and LUSC tissues sections. The images were acquired using the same exposure time and are shown on the same scale for each lectin in the Cy3- and DAPI-merge channel. (F) The relative expression level of the core fucosylation glycans in PCTs and LUSC tissues. The fluorescence intensities were acquired by ImageJ software.



of trypsin. After the temperature of mixture restored to room temperature, 2  $\mu\text{L}$  PNGase F was added and incubated at 37  $^{\circ}\text{C}$  overnight to release the *N*-linked glycans from the glycopeptides. Finally, the filtrates that contained peptides and *N*-linked glycans were collected by centrifugation, and the released glycans were purified with HyperSep Hypercarb SPE cartridges (25 mg, 1 mL; Thermo Scientific) according to the manufacturer's recommendation. The glycans were eluted by 0.5 mL of elution solution (50% (v/v) acetonitrile with 0.1% (v/v) TFA). The purified glycans were collected and lyophilized.

## 2.8 Characterization of the *N*-linked glycans by MALDI-TOF/TOF-MS

The purified glycans were characterized by MALDI-TOF/TOF-MS (UltrafleXtreme, Bruker Daltonics). Glycans were resuspended in 10  $\mu\text{L}$  of methanol, and 1  $\mu\text{L}$  was spotted directly on the MTP AnchorChip sample target and dried. Then 1  $\mu\text{L}$  of 10 mg  $\text{mL}^{-1}$  DHB in 50% (v/v) methanol solution was spotted to the recrystallized glycans. Mass calibration was performed using peptide calibration standards (250 calibration points; Bruker). Measurements were taken in positive-ion mode,  $m/z$  data were generated and analyzed using FlexAnalysis and GlycoWorkbench software, respectively. Relative intensity was calculated by dividing the intensity of a given type of glycan by the highest glycans intensity of its MS spectra.

## 3. Results

### 3.1 The alterations of glycopatterns in LUSC tissues versus PCTs

To identify the abnormal glycopatterns associated with LUSC, the lectin microarrays were utilized to compare the glycopatterns between the paired PCTs and LUSC tissues. The layout of the lectin microarrays and one pair of Cy3-labeled proteins from PCTs and LUSC tissues bound to the lectin microarrays were shown in Fig. 1A and B. The generated data from each sample was imported into EXPANDER software and further analyzed using a hierarchical clustering method to exhibit the overview of the glycopatterns among all the paired tissue samples (Fig. 1C). By the paired *t*-test analysis, it was found that the Gal $\beta$ -1,3/4 GlcNAc, Sia $\alpha$ -2-3Gal binder MAL-I exhibited significantly increased the normalized fluorescent intensities (NFIs) in the LUSC tissues against PCTs ( $P < 0.05$ ) among all the paired tissue samples, and the  $\alpha$ -D-Man, Fuc $\alpha$ -1,6GlcNAc (core fucose),  $\alpha$ -D-Glc binder LCA and Fuc $\alpha$ -1,6GlcNAc binder PSA showed significantly increased the NFIs among six paired tissue samples (Table 1). However, the NFIs of other lectins were not significantly different between LUSC tissues and PCTs. Therefore, the abnormal expression of Fuc $\alpha$ -1,6GlcNAc structure was perceived as the most important changes between LUSC tissues and PCTs.

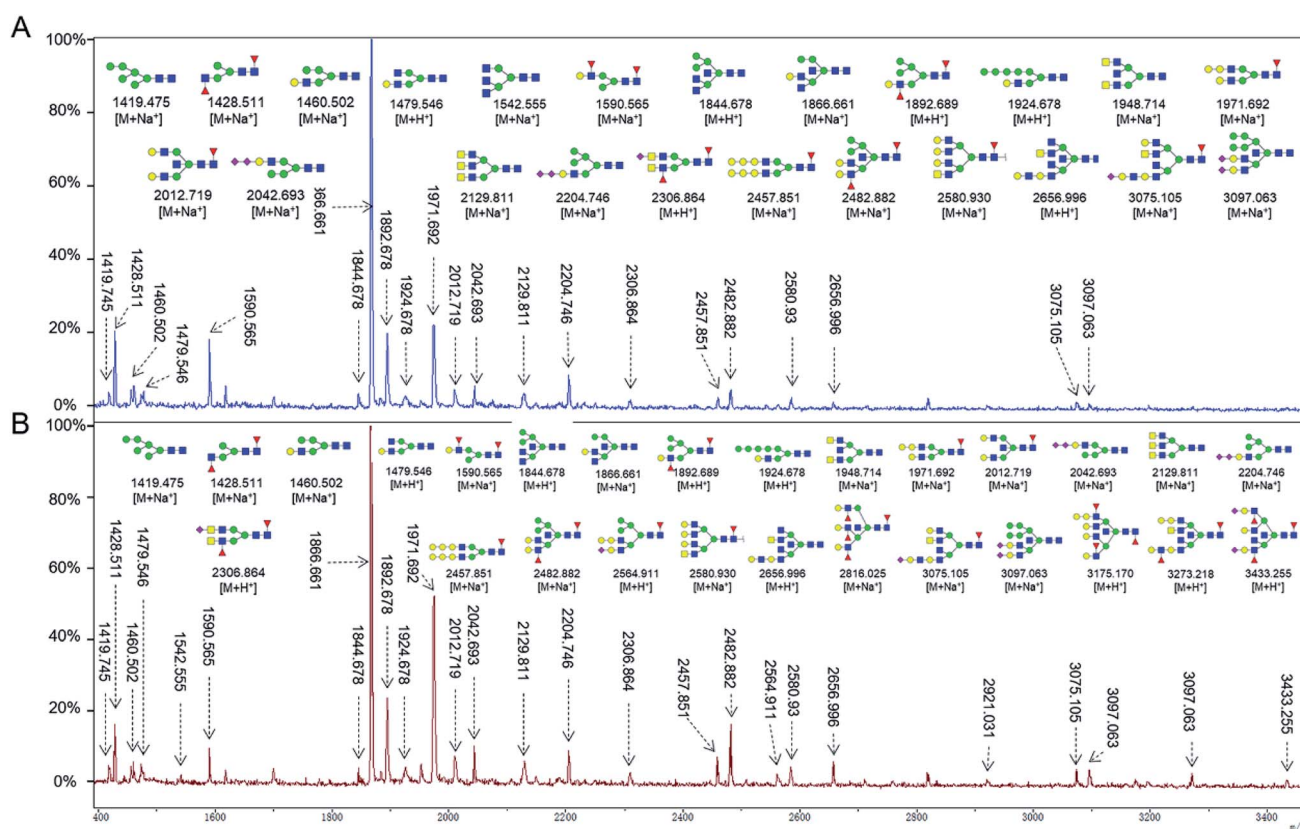


Fig. 3 MALDI-TOF/TOF-MS spectra of the purified *N*-linked glycans from the pooled tissue samples of PCT (A) and LUSC (B), respectively. Detailed glycan structures were analyzed using the GlycoWorkbench software. Proposed structures and their  $m/z$  values were shown for each peak. Blue square = GlcNAc, green circle = Man, yellow circle = Gal, yellow square = GalNAc, purple diamond = NeuAc, red triangle = Fuc.



Table 2 The proposed *N*-linked glycan peaks detected in the present study<sup>a</sup>

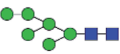
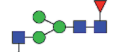
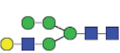

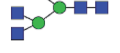


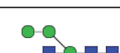


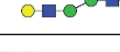
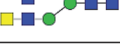
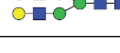



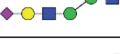
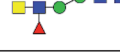
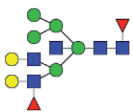
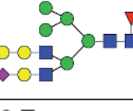
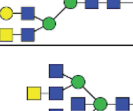
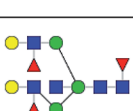
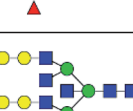
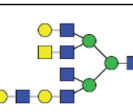
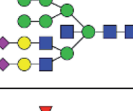
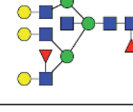
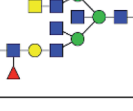
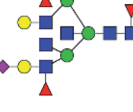
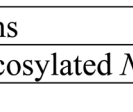
No.	Ion	Proposed glycan structure <sup>b</sup>	Calculated m/z	Relative intensity <sup>c</sup>	
				PCTs	SCC
1	Na		1419.475	0.058	0.072
2	Na		1428.511	0.219	0.186
3	Na		1460.502	0.075	0.053
4	H		1479.546	0.053	0.055
5	Na		1542.555	0.038	0
6	Na		1590.565	0.194	0.232
7	H		1844.678	0.056	0.068
8	Na		1866.661	1.000	1.000
9	H		1892.689	0.210	0.205
10	H		1924.678	0.048	0.070
11	Na		1948.714	0.036	0.054
12	Na		1971.692	0.233	0.505
13	Na		2012.719	0.065	0.101
14	Na		2042.693	0.063	0.070
15	H		2129.811	0.056	0.089
16	Na		2204.746	0.095	0.115
17	H		2306.864	0.031	0.046
18	Na		2457.851	0.044	0.026





Table 2 (Contd.)

No.	Ion	Proposed glycan structure <sup>b</sup>	Calculated m/z	Relative intensity <sup>c</sup>	
				PCTs	SCC
19	Na		2482.882	0.064	0.087
20	H		2564.911	0	0.038
21	Na		2580.93	0.043	0.042
22	H		2656.996	0.033	0.062
23	Na		2816.025	0	0.050
24	Na		2921.031	0	0.029
25	Na		3075.105	0.029	0.057
26	Na		3097.063	0.022	0.046
27	H		3175.17	0	0.028
28	H		3273.218	0	0.030
29	H		3433.255	0	0.031
Totally N-glycans				2.766	3.446
Fucosylated N-glycans				1.131	1.663
The percentage of fucosylated N-glycans				40.9%	48.3%

<sup>a</sup> Monosaccharides are represented according to MS-tools from the GlycoWorkbench software (GlcNAc, blue square; Man, green circle; Gal, yellow circle; Fuc, red triangle; NeuAc, purple diamond). <sup>b</sup> The proposed glycan structure. <sup>c</sup> The relative intensity was calculated by dividing the intensity of a given type of glycan by the highest glycans intensity of its MS spectra.



### 3.2 Validation of the differences glycopatterns between LUSC tissues and PCTs

According to the results of the lectin microarrays, there was an abnormal expression of Fuc $\alpha$ -1,6GlcNAc structure recognized specifically by PSA and LCA in LUSC tissues. SDS-PAGE and lectin blotting analysis were performed with silver staining, Cy5-labeled PSA and LCA staining to rapidly validate the target glycan structures, respectively (Fig. 2A). The results of SDS-PAGE demonstrated that the protein bands from each paired tissue sample were similar. The results of the lectin blotting analysis showed that there was only one major band with molecular weight of approximately 53 kDa that showed an apparently increased fluorescence intensities in LUSC tissues compared with PCTs (Fig. 2B). Besides, the increased expression level of Fuc $\alpha$ -1,6GlcNAc structure in LUSC tissues was also verified at the genetic level. FUT8 as the only enzyme responsible for  $\alpha$ 1,6-linked core fucosylation by adding fucose to the innermost GlcNAc residue of an *N*-linked glycan was detected using qRT-PCR. The data showed that the gene expression level of FUT8

was significantly increased in LUSC tissues compared to PCTs (Fig. 2C). These results were basically consistent with the results of lectin microarrays.

### 3.3 Expression and distribution of the specific glycan in the tissue sections

To further validate and assess the expression and distribution of the Fuc $\alpha$ -1,6GlcNAc in PCTs and LUSC tissues, fluorescence-based lectin histochemistry was performed with PSA lectins. The hematoxylin–eosin (H&E) pathological staining were performed to verify the LUSC tissue (Fig. 2D). The result of H&E illustrated that nuclear atypia of LUSC tissues was more clear than that of PCTs. Lectin histochemistry indicated that PSA strongly bind to the cytoplasm and the membrane of lung cells (Fig. 2E). As a result, it is obvious that the fluorescence signal intensity of PSA was significantly increased in LUSC tissues compared to PCTs (Fig. 2E and F). The result demonstrated that the core fucosylated glycan increased on the surface and

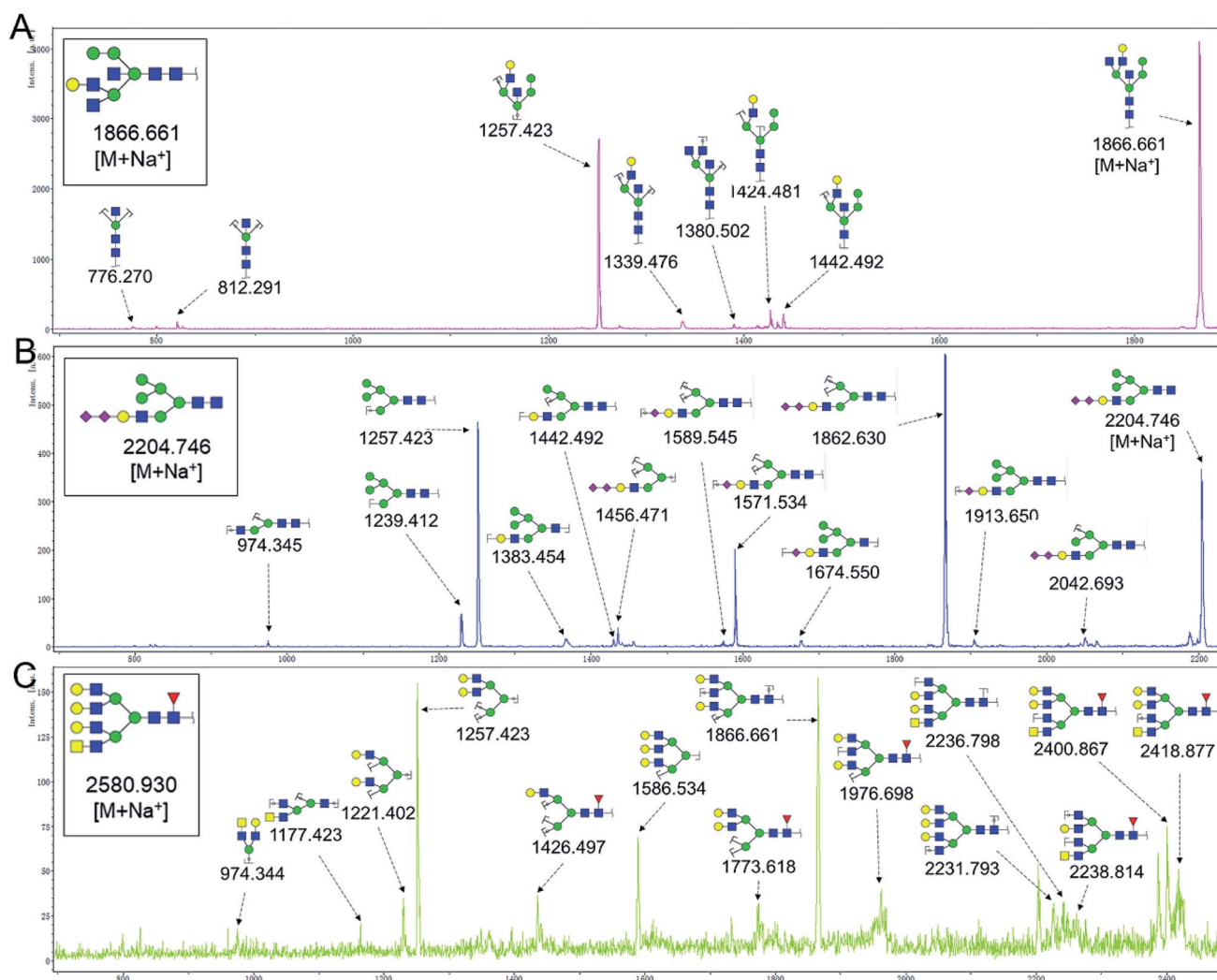


Fig. 4 MALDI-TOF/TOF MS/MS analyzing the *N*-glycan precursor ion from MS spectra. With example, the three *N*-glycan peaks (A) *m/z* 1866.661, (B) 2204.746, and (C) 2580.930, subjected to MS/MS analysis.





cytoplasm of lung cells when LUSC occurred. And the result was in accord with the above experiments and verifications.

### 3.4 Alterations of fucosylated *N*-linked glycan profiles in LUSC tissues versus PCTs

To obtain detail structural information of glycoproteins from the tumor and PCTs. The *N*-linked glycans were released from glycoproteins by PNGase F and identified by MALDI-TOF/TOF-MS. The identified *N*-linked glycans and their proposed structures from the pooled tissue samples of LUSC and PCTs were shown in Fig. 3 and Table 2. A total of 23 and 28 *N*-linked glycans were identified and annotated, respectively. Of these, 22 *N*-linked glycans (*e.g.*, *m/z* 1419.475, 1428.511 and 1460.502) were observed both in PCTs and LUSC tissues, while one *N*-linked glycans (*m/z* 1542.555) detected only in PCTs and six *N*-linked glycans (*e.g.*, *m/z* 2564.911, 2816.025, and 2921.031) detected only in LUSC tissues. The MS/MS spectra of the precursor ions *m/z* 1866.661, 2204.746, and 2580.930 were illustrated in Fig. 4A–C.

Focusing on the fucosylated *N*-glycans, it is noticeable that there were 10 and 15 fucosylated *N*-linked glycans were detected in PCTs and LUSC tissues, respectively. Of these fucosylated *N*-glycans, there was an overlap of 10 fucosylated *N*-glycan peaks (*e.g.*, *m/z* 1428.51, 1590.565 and 1892.689) between PCTs and LUSC tissues. Besides, five fucosylated *N*-glycans (including *m/z* 2564.911, 2816.025, 3175.17, 3273.218, and 3433.255) were unique to LUSC tissues. In fact, not only the numbers but also the relative intensity of fucosylated glycans were shown significant increasing in the LUSC tissues compared with that in PCTs. The sum relative intensity of fucosylated glycans were increased from 1.131 in PCTs to 1.663 in LUSC tissues. And the proportion of the fucosylated *N*-linked glycans was significantly increased from 40.9% (PCTs) to 48.3% (LUSC).

## 4. Discussion

Glycosylation involve in a wide range of biological processes including cellular communication, adhesion, interaction, malignant transformation and metastasis.<sup>27,28</sup> The synthesis of glycan is a complex process with the coordination of multiple organelles and strictly regulated by a set of enzymes, which result innumerable possibilities for branching and anomeric linkage.<sup>13,29</sup> Given the complexity of protein glycosylation and its fundamental effects on a variety of biological processes, it is no doubt that aberrant glycosylation not only represents a characteristic of cancer, but also significantly impact the biology of cells, thus analysis of the abnormal glycopatterns in malignant tissues are contribute to understand the mechanisms of cancerization.<sup>13,30–33</sup>

Our previous study investigated the glycopatterns of serum proteins in non-small cell lung cancer (NSCLC) patients at different stages using a lectin microarray, and systematically compare the alterations of serum glycopatterns between NSCLC patients and healthy controls. There were 18 lectins (*e.g.*, AAL, Jacalin, GSL-I and DBA) and 16 lectins (*e.g.*, Jacalin, HHL, and PHA-E + L) exhibited significantly alterations of serum glycopatterns in lung adenocarcinoma and LUSC patients compared to healthy group, respectively.<sup>34</sup> Meanwhile, the levels of core fucosylation was elevated and showed positive correlated with the development of lung

adenocarcinoma, but not in LUSC patients.<sup>34</sup> In the present study, the different glycopatterns between LUSC tissues and PCTs were detected by the lectin microarrays. The MAL-I, LCA and PSA showed significantly increased NFIs in the LUSC tissues. And the level of the core fucosylation identified by PSA and LCA and FUT8 was significantly elevated in LUSC tissues in this study. Previous studies also showed that the expression level of FUT8 was elevated in NSCLC tissues and further indicated that up-regulation of FUT8 contributes to tumor progression through multiple mechanisms.<sup>22,35,36</sup> The elevated core fucosylation and transcription of FUT8 have been also observed in sera of hepatocellular carcinoma, prostate and ovarian cancer patients.<sup>37–39</sup>

In conclusion, the present study systematically investigated the glycopatterns between LUSC tissues and PCTs. The glycopattern of core fucosylation was significantly increased in LUSC tissues compared with PCTs. Furthermore, the numbers of *N*-glycans with fucosylation were increased remarkably in LUSC tissues, five fucosylated *N*-glycans were detected only in LUSC tissues, and the abundance of fucosylated *N*-glycans was increased from 40.9% (PCTs) to 48.3% (LUSC). Our data provided useful information in order to elucidate the molecular mechanisms of LUSC and develop new treatment strategies. However, the association among abnormal glycosylation and malignant transformation, infiltration, and migration are still needed to further explore.

## Funding

This work is supported by National Natural Science Foundation of China (Grant No. 81871955) and the Northwest University Doctorate Dissertation of Excellence Funds (Grant No. YYB17018).

## Conflicts of interest

The authors declare that there are no conflicts of interest.

## Abbreviations

FUT8	Fucosyltransferase 8
HCA	Hierarchical cluster analysis
H&E	Hematoxylin–eosin
LCA	<i>Lens culinaris</i> agglutinin
LUSC	Lung squamous cell carcinoma
MAL-I	<i>Maackia amurensis</i> lectin I
NSCLC	Non-small cell lung cancer
PCTs	Pericarcinomatous tissues
PSA	<i>Pisum sativum</i> agglutinin
qRT-PCR	Quantitative real-time polymerase chain reaction

## References

- 1 F. Bray, J. Ferlay, I. Soerjomataram, R. L. Siegel, L. A. Torre and A. Jemal, *Ca-Cancer J. Clin.*, 2018, **68**, 394–424.
- 2 W. D. Travis, E. Brambilla, A. G. Nicholson, Y. Yatabe, J. H. M. Austin, M. B. Beasley, L. R. Chirieac, S. Dacic,



- E. Duhig, D. B. Flieder, K. Geisinger, F. R. Hirsch, Y. Ishikawa, K. M. Kerr, M. Noguchi, G. Pelosi, C. A. Powell, M. S. Tsao and I. Wistuba, *J. Thorac. Oncol.*, 2015, **10**, 1243–1260.
- 3 W. D. Travis, *Clin. Chest. Med.*, 2011, **32**, 669–692.
- 4 J. Brahmer, K. L. Reckamp, P. Baas, L. Crino, W. E. Eberhardt, E. Poddubskaya, S. Antonia, A. Pluzanski, E. E. Vokes, E. Holgado, D. Waterhouse, N. Ready, J. Gainor, O. Aren Frontera, L. Havel, M. Steins, M. C. Garassino, J. G. Aerts, M. Domine, L. Paz-Ares, M. Reck, C. Baudelet, C. T. Harbison, B. Lestini and D. R. Spigel, *N. Engl. J. Med.*, 2015, **373**, 123–135.
- 5 S. Senoo, K. Ninomiya, K. Hotta and K. Kiura, *Int. J. Clin. Oncol.*, 2019, **24**, 461–467.
- 6 T. Tamura, Y. Kato, K. Ohashi, K. Ninomiya, G. Makimoto, H. Gotoda, T. Kubo, E. Ichihara, T. Tanaka, K. Ichimura, Y. Maeda, K. Hotta and K. Kiura, *Biochem. Biophys. Res. Commun.*, 2018, **495**, 360–367.
- 7 H. Isozaki, K. Hotta, E. Ichihara, N. Takigawa, K. Ohashi, T. Kubo, T. Ninomiya, K. Ninomiya, N. Oda, H. Yoshioka, H. Ichikawa, M. Inoue, I. Takata, T. Shibayama, S. Kuyama, K. Sugimoto, D. Harada, S. Harita, T. Sendo, M. Tanimoto and K. Kiura, *Clin. Lung Cancer*, 2016, **17**, 602–605.
- 8 K. T. Bui, W. A. Cooper, S. Kao and M. Boyer, *J. Clin. Med.*, 2018, **7**, E192.
- 9 T. Shukuya, T. Takahashi, R. Kaira, A. Ono, Y. Nakamura, A. Tsuya, H. Kenmotsu, T. Naito, K. Kaira, H. Murakami, M. Endo, K. Takahashi and N. Yamamoto, *Cancer Sci.*, 2011, **102**, 1032–1037.
- 10 X. Song, X. Han, F. Yu, X. Zhang, L. Chen and C. Lv, *Theranostics*, 2018, **8**, 2217–2228.
- 11 X. Zhang, N. He, Y. Huang, F. Yu, B. Li, C. Lv and L. Chen, *Sens. Actuators, B*, 2019, **282**, 69–77.
- 12 M. Cumberbatch, X. Tang, G. Beran, S. Eckersley, X. Wang, R. P. Ellston, S. Dearden, S. Cosulich, P. D. Smith, C. Behrens, E. S. Kim, X. Su, S. Fan, N. Gray, D. P. Blowers, I. I. Wistuba and C. Womack, *Clin. Cancer Res.*, 2014, **20**, 595–603.
- 13 S. R. Stowell, T. Ju and R. D. Cummings, *Annu. Rev. Pathol.: Mech. Dis.*, 2015, **10**, 473–510.
- 14 C. Reily, T. J. Stewart, M. B. Renfrow and J. Novak, *Nat. Rev. Nephrol.*, 2019, **15**, 346–366.
- 15 Q. Yang, R. Zhang, H. Cai and L. X. Wang, *J. Biol. Chem.*, 2017, **292**, 14796–14803.
- 16 Y. Wang, T. Fukuda, T. Isaji, J. Lu, W. Gu, H. H. Lee, Y. Ohkubo, Y. Kamada, N. Taniguchi, E. Miyoshi and J. Gu, *Sci. Rep.*, 2015, **5**, 8264.
- 17 M. Ueda, Y. Kamada, S. Takamatsu, M. Shimomura, T. Maekawa, T. Sobajima, H. Fujii, K. Nakayama, K. Nishino, M. Yamada, Y. Kobayashi, T. Kumada, T. Ito, H. Eguchi, H. Nagano and E. Miyoshi, *Pancreatol.*, 2016, **16**, 238–243.
- 18 J. Ma, M. Sanda, R. Wei, L. Zhang and R. Goldman, *J. Proteomics*, 2018, **189**, 67–74.
- 19 H. Fujii, S. Shinzaki, H. Iijima, K. Wakamatsu, C. Iwamoto, T. Sobajima, R. Kuwahara, S. Hiyama, Y. Hayashi, S. Takamatsu, N. Uozumi, Y. Kamada, M. Tsujii, N. Taniguchi, T. Takehara and E. Miyoshi, *Gastroenterology*, 2016, **150**, 1620–1632.
- 20 M. Noda, H. Okayama, Y. Kofunato, S. Chida, K. Saito, T. Tada, M. Ashizawa, T. Nakajima, K. Aoto, T. Kikuchi, W. Sakamoto, H. Endo, S. Fujita, M. Saito, T. Momma, S. Ohki and K. Kono, *PLoS One*, 2018, **13**, e0200315.
- 21 L. Veillon, C. Fakih, H. Abou-El-Hassan, F. Kobeissy and Y. Mechref, *ACS Chem. Neurosci.*, 2018, **9**, 51–72.
- 22 C. Y. Chen, Y. H. Jan, Y. H. Juan, C. J. Yang, M. S. Huang, C. J. Yu, P. C. Yang, M. Hsiao, T. L. Hsu and C. H. Wong, *Proc. Natl. Acad. Sci. U. S. A.*, 2013, **110**, 630–635.
- 23 J. Shu, H. Yu, X. Li, D. Zhang, X. Liu, H. Du, J. Zhang, Z. Yang, H. Xie and Z. Li, *Oncotarget*, 2017, **8**, 35718–35727.
- 24 Y. Qin, Y. Zhong, M. Zhu, L. Dang, H. Yu, Z. Chen, W. Chen, X. Wang, H. Zhang and Z. Li, *J. Proteome Res.*, 2013, **12**, 2742–2754.
- 25 H. Yu, M. Zhu, Y. Qin, Y. Zhong, H. Yan, Q. Wang, H. Bian and Z. Li, *J. Proteome Res.*, 2012, **11**, 5277–5285.
- 26 J. Shu, H. Yu, H. Du, J. Zhang, K. Zhang, X. Li, H. Xie and Z. Li, *Cancer Biomarkers*, 2018, **22**, 669–681.
- 27 J. Shu, L. Dang, D. Zhang, P. Shah, L. Chen, H. Zhang and S. Sun, *FEBS J.*, 2019, **286**, 1594–1605.
- 28 M. Dalziel, M. Crispin, C. N. Scanlan, N. Zitzmann and R. A. Dwek, *Science*, 2014, **343**, 1235681.
- 29 K. W. Moremen, M. Tiemeyer and A. V. Nairn, *Nat. Rev. Mol. Cell Biol.*, 2012, **13**, 448–462.
- 30 L. Oliveira-Ferrer, K. Legler and K. Milde-Langosch, *Semin. Cancer Biol.*, 2017, **44**, 141–152.
- 31 J. H. Rho, J. J. Ladd, C. I. Li, J. D. Potter, Y. Zhang, D. Shelley, D. Shibata, D. Coppola, H. Yamada, H. Toyoda, T. Tada, T. Kumada, D. E. Brenner, S. M. Hanash and P. D. Lampe, *Gut*, 2018, **67**, 473–484.
- 32 X. Liu, H. Yu, Y. Qiao, J. Yang, J. Shu, J. Zhang, Z. Zhang, J. He and Z. Li, *EBioMedicine*, 2018, **28**, 70–79.
- 33 A. Silsirivanit, *Adv. Clin. Chem.*, 2019, **89**, 189–213.
- 34 Y. Liang, P. Han, T. Wang, H. Ren, L. Gao, P. Shi, S. Zhang, A. Yang, Z. Li and M. Chen, *Clin. Proteomics*, 2019, **16**, 20.
- 35 R. Honma, I. Kinoshita, E. Miyoshi, U. Tomaru, Y. Matsuno, Y. Shimizu, S. Takeuchi, Y. Kobayashi, K. Kaga, N. Taniguchi and H. Dosaka-Akita, *Oncology*, 2015, **88**, 298–308.
- 36 C. F. Tu, M. Y. Wu, Y. C. Lin, R. Kannagi and R. B. Yang, *Breast Cancer Res.*, 2017, **19**, 111.
- 37 W. R. Alley Jr, J. A. Vasseur, J. A. Goetz, M. Svoboda, B. F. Mann, D. E. Matei, N. Menning, A. Hussein, Y. Mechref and M. V. Novotny, *J. Proteome Res.*, 2012, **11**, 2282–2300.
- 38 X. Wang, J. Chen, Q. K. Li, S. B. Peskoe, B. Zhang, C. Choi, E. A. Platz and H. Zhang, *Glycobiology*, 2014, **24**, 935–944.
- 39 A. Mehta, P. Norton, H. Liang, M. A. Comunale, M. Wang, L. Rodemich-Betesh, A. Koszycki, K. Noda, E. Miyoshi and T. Block, *Cancer Epidemiol., Biomarkers Prev.*, 2012, **21**, 925–933.

